Universiteit
Leiden
The Netherlands

Towards High-Speed Scanning Tunneling Microscopy

Tabak, F.C.

Citation

Tabak, F. C. (2013, June 5). *Towards High-Speed Scanning Tunneling Microscopy*. *Casimir PhD Series*. Retrieved from https://hdl.handle.net/1887/20925

Version:	Not Applicable (or Unknown)
License:	Leiden University Non-exclusive license
Downloaded from:	https://hdl.handle.net/1887/20925

Note: To cite this publication please use the final published version (if applicable).

Cover Page

Universiteit Leiden

The handle http://hdl.handle.net/1887/20925 holds various files of this Leiden University dissertation.

Author: Tabak, F.C.
Title: Towards high-speed scanning tunneling microscopy
Issue Date: 2013-06-05

Chapter 2

MEMS-based STM scanners

In this chapter, we describe how miniaturised STM scanners can be beneficial to "conventional" piezo-element based STM scanners. We propose to use Micro-Electro Mechanical Systems (MEMS) to increase the speed of STM scanners beyond the possibilities of classical piezo-element configurations. MEMS can be designed to perform scanning motion, including out-of-plane feedback corrections, and can have extremely high resonance frequencies (1 MHz range), combined with a very low mass (picograms). These are beneficial properties in STM and AFM scanning. Several directions within MEMS STM have been investigated before, which are discussed in section 2.4. A general MEMS introduction is given, followed by an introduction to the STM-specific structures and a mathematical analysis of the advantages of MEMS STM scanners over conventional piezo-based STM scanners.

2.1 MEMS introduction

Micro-Electro Mechanical Systems (MEMS) are devices with micrometer-sized features that perform electronic and mechanical actions. They are fabricated with modified versions of the techniques developed for the micro-electronics industry. MEMS are widely used as motion sensors for instance in car airbags, in Wii controllers [49] and in smartphones.

2.1.1 Working principle

MEMS devices are similar to well-known micro-electronic circuits in the sense that they are "printed" on a chip by a lithographic fabrication process. The difference with regular electronic circuits is, that (part of) a MEMS can also perform motion. The simplest actuation mechanism exploited in a MEMS consists of two conductive beams, which thus form a capacitor. This structure is shown schematically in figure 2.1. One of the beams is fixed to the wafer;

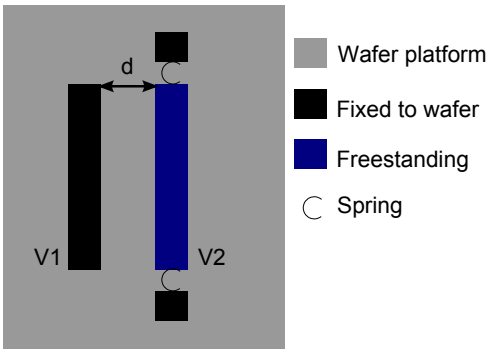

Figure 2.1: *The working principle of a MEMS device (top view). The left beam is fixed to the substrate, whereas the right beam is held by two springs. By applying a voltage difference between the two beams, the right beam can be actuated, as dictated by the electrostatic force and Hooke's law.*

the other one is freestanding over the surface and is held by two springs. The capacitance C of this system is given by:

$$C = \frac{\epsilon_0 A}{d} \tag{2.1}$$

Where A is the surface overlap between the two beams and d the distance between them. By applying a voltage difference V between the two beams, we exert a force on the beams, which is given by [50]:

$$F = \frac{1}{2}V^2\frac{\partial C(d)}{\partial d} = -\frac{1}{2}\frac{\epsilon_0 A V^2}{d^2} \tag{2.2}$$

The force on the beams results in a displacement x of the freestanding beam. This is the basic principle of electrostatic actuation. According to Hooke's law (for small displacements and therefore a constant stiffness), in equilibrium, the force F exerted by the voltage difference (equation 2.2) equals the force $-kx$ exerted by the springs that hold the freestanding actuator with an effective spring constant k. Thus, we can actuate a MEMS device by keeping the potential of one of the beams constant (i.e. ground) and varying the voltage on the other beam. From eq. 2.2 it follows that the displacement of the MEMS membrane as a function of voltage is determined by the spring constant, the capacitive area and the distance between the plates. During the actuation of the MEMS device, the separation of the two plates changes, so equation 2.2 has to be written as:

$$F == -\frac{1}{2}\frac{\epsilon_0 A V^2}{(d_0 - x)^2} \tag{2.3}$$

Later (in section 2.3.1) we will discuss how the natural resonance frequency of the MEMS device also depends on k, and how this leads to a trade-off between actuation range and resonance frequency.

2.1.2 Failure modes of MEMS devices

While some MEMS devices are used in commercial applications, many MEMS designs are never commercialized. Besides the commercial risks that are involved with starting an expensive batch project, there is a persisting problem: MEMS devices suffer from a wide variety of failure modes that are not so well characterised, let alone solved [51, 52]. Some of these failure modes can also affect the MEMS STM scanner: (1) stiction, (2) charging of the dielectric and (3) contamination. Stiction may occur in a MEMS system where there is a small gap between two structural parts, of which at least one is mobile. Surface forces can be dominant in structures of very small size such as MEMS and cause microscopic structures to stick together. Stiction may occur because of capillary forces, Van der Waals interaction, chemical bonding, and Casimir forces. This is an important issue in the drying process after the release etch during the manufacturing of the device, and it is also important in STM applications. Once stuck, the surfaces can not be made to release by applying actuation voltages, for the simple reason that the electrostatic forces in these devices are *always* attractive. Since the electrostatic force increases as d decreases, these devices exhibit an intrinsic pull-in instability beyond a certain actuation voltage. The combination of this pull-in instability with the stiction problem imposes very stringent limits on the use of MEMS devices. In-use pull-in events along with the corresponding pull-out voltages are described by the Van Spengen model [53, 54]. For the MEMS SPM scanner, we want to avoid sticking surfaces to each other during actuation, i.e. we want to prevent a pull-in event. Pull-in of the membrane will occur when the membrane has travelled 1/3 of the gap between membrane and actuator, regardless of the exact geometry of the device, as can be calculated analytically by combining equation 2.2 with Hooke's law and solving this for $dV/dx = 0$. Pull-in events are an important effect when designing a MEMS STM or AFM scanner, since this limits the accessible scan range to 1/3 of the spacing between scanning membrane and actuator. MEMS scanners should be designed carefully to optimise the maximum actuation voltage to the maximum scan

range. If the actuation voltage at which the pull-in event will occur is too small, it will be difficult to actuate the MEMS scanner precisely enough to obtain atomic resolution. If the actuation voltage at which the pull-in event occurs is higher than the voltage range of the STM voltage drivers, the maximum scan range will be reduced to a range below 1/3 of the gap between membrane and actuator.
The voltage at which the pull-in event occurs can be influenced by electrostatic charging. Charging of the dielectric can occur below and at the edges of the actuator plate. This will cause shifting (reduction) of the pull-in voltage and lead to erratic behaviour of the device. Charging typically poses problems when actuating MEMS structures at higher voltages (>80V). For lower voltages, charging is usually not problematic [55].
Last but not least, MEMS can suffer from contamination. For most commercial applications, MEMS need special packaging. Standard packaging as used for IC circuits usually is not an option for MEMS, since MEMS sensors need to have a 'window' to the world. This also goes for our MEMS SPM scanner. The devices presented in this thesis have all been used without any packaging. Contamination was found to reduce the lifetime of the scanners to a few months, after which they were covered with a significant number of dust particles. This lifespan, after which a scanner needs to be exchanged, is reasonable for STM scanners, since there are other components in SPM experiments, such as the tip or the sample, that usually require attention more frequently. A MEMS z-actuator could be designed to be exchangeable in a fashion similar to commercially available AFM cantilevers.

2.1.3 Fabrication

Micro-electro mechanical systems are fabricated in lithographic processes by subsequent steps of deposition of silicon and masks, patterning and etching. We acquired our MEMS devices via two commercial multi-user processes, offered by the company MEMSCAP [56]: the PolyMUMPS process and the SOIMUMPS process. Even though commercial MEMS processes necessarily introduce design limitations, we have made use of them in order to save time, since it was not necessary to develop our own custom lithography process. I will explain these processes briefly; more information can be found in the PolyMUMPS design handbook [57] and the SOIMUMPS design handbook [58].

PolyMUMPS process

With the polyMUMPS process (figures 2.2 and 2.3), one can design MEMS with one fixed (polycrystalline silicon) layer and two freestanding polysilicon layers, optionally covered with gold pads. The MEMS fabrication starts with 150 mm n-type Si(100) wafers with $1 - 2\Omega cm$ resistivity. First, the wafer is doped (this is to prevent charging), followed by the deposition of a silicon-nitride layer which acts as electrical isolation between the wafer and the electrostatically actuated devices on top. Then, the first polysilicon layer is deposited. This layer is patterned by photolithography: it is covered with a layer of photoresist, which is then illuminated using a mask (carrying the desired design of this layer). The layer is now developed, i.e. the part of the photoresistive layer which is not illuminated through the mask is removed. This is followed by an etching step in which the exposed polysilicon is etched away, simultaneously removing the remaining part of the layer of photoresist. This leaves the wafer covered with a silicon layer with the same design as the mask. This procedure is repeated two more times to deposit the next two silicon layers (see figure 2.2). The standard thicknesses are 500 nm for the fixed Poly0 layer, 2.0 μm for the Poly1 layer and 1.5 μm for the Poly2 layer. The Poly1 and Poly2 silicon layers can be made freestanding. This is achieved by the deposition of two oxide layers between the three silicon layers. The oxide layers are etched away completely at the end of the fabrication process, leaving those parts of the second and third silicon layer freestanding that had been deposited on oxide (figure 2.3). On top of the silicon layers, gold can be deposited, facilitating electrical connections to the MEMS structures. Making use of the three layers, MEMS devices can be designed that can move in x, y and/or z directions.

SOIMUMPS process

The SOIMUMPS process is a Silicon-On-Insulator micromachining process. The process starts with a 400 μm silicon substrate that carries a 1 μm oxide layer and either a 10 μm or a 25 μm silicon layer, depending on the specifications of the user. First, a metal layer is deposited and patterned. Then, the silicon layer is lithographically patterned and etched with a DRIE (deep reactive ion etch) process. After this, an etch is done from the rear side of the substrate, allowing for through-etches and thus creating completely freestanding structures. Finally, an etch step is performed that removes the insulating oxide layer on the desired places, releasing structures that are designed to be

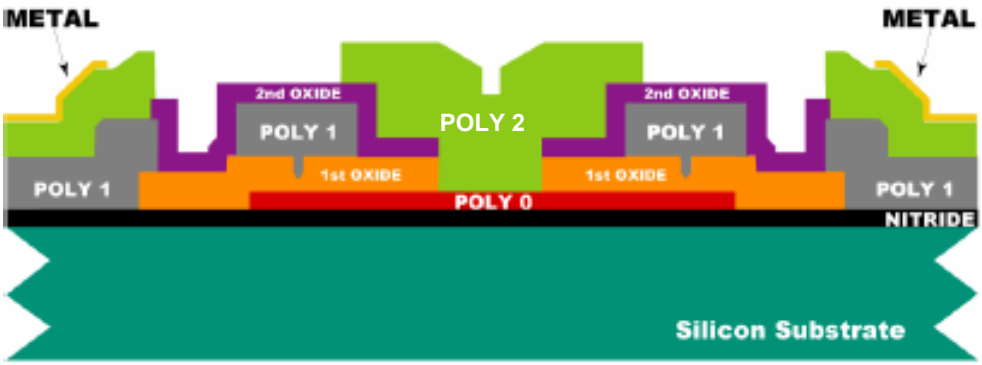

Figure 2.2: *Schematic drawing of the different deposited layers in the PolyMUMPS process. The structure consists of the silicon substrate, a nitride layer, three polysilicon layers (poly0, poly1 and poly2), a top metal layer and two sacrificial oxide layers. Reprinted with permission from [57].*

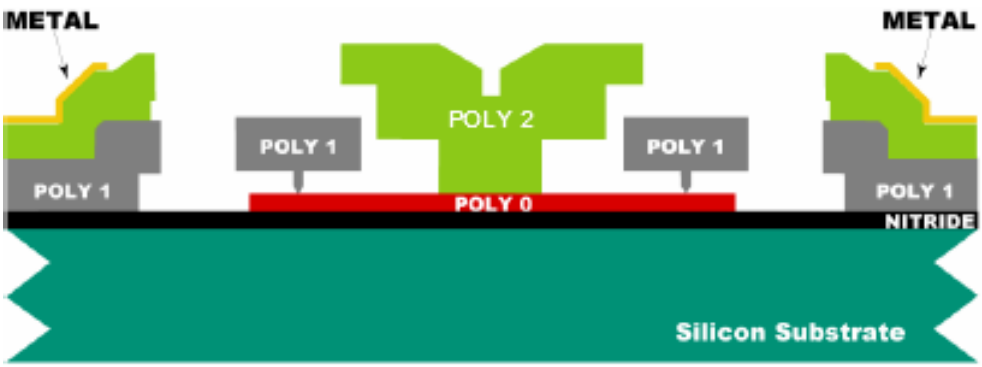

Figure 2.3: *Schematic drawing of the final structure in the PolyMUMPS process. After removal of the two sacrificial oxide layers, the poly1 and poly2 layers can now have moving parts. The top metal is used for contacting the structures. Reprinted with permission from [57].*

freestanding over the wafer.

2.2 Introduction to MEMS STM scanners

Using the two processes described above in section 2.1.3, we have fabricated various types of MEMS STM scanners. The following sections cover the properties of the MEMS STM scanners; here, the structures are introduced. Most scanners were produced with the PolyMUMPS process, unless otherwise

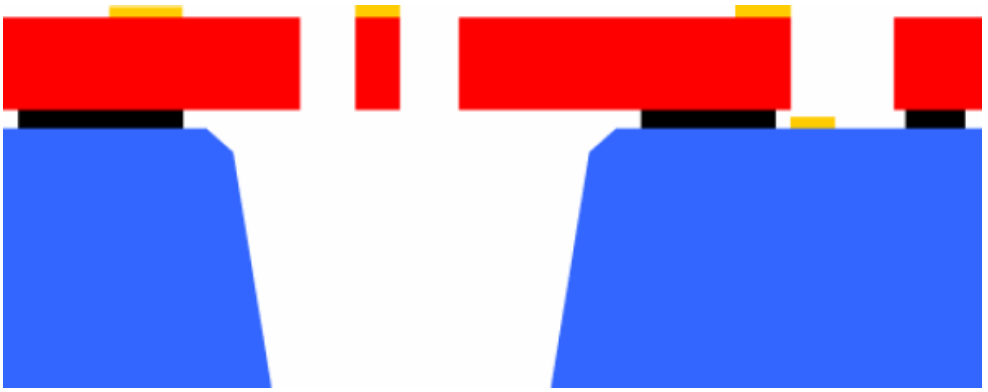

Figure 2.4: *Schematic drawing of a structure made in the SOIMUMPS process. The structure consists of the substrate (blue), an insulating oxide layer (black), a silicon structure (red) and a contacting metal (yellow). The oxide, silicon structure and metal can be patterned and the silicon structures can be freestanding over a hole in the substrate, created by a through-etch. Reprinted with permission from [58].*

stated. The moving parts were made out of the Poly1 layer and thus have a thickness of 2 μm.
The basic scanner design that we have used is shown in the left panel of figure 2.5. The heart of this scanner is a central membrane; this is the part that performs the high-speed, out-of-plane motion. It is supported by four springs which all have a 90° elbow to optimize thermal stability. The springs are fixed at the four supports. The width and length of the springs and the size of the membrane can be chosen to tune the resonance frequency and actuation properties of the scanner. The actuation plate is located below the scanning membrane. By applying a voltage difference between the scanning membrane and the actuation plate, the membrane is displaced over a well-defined distance governed by equation 2.3. The lines for electrical connections are led to the gold contact pads, several hundred micrometers away. Thin (gold) wires can then be wirebonded to these pads, to connect the scanner to the outside world. Several MEMS z-actuators are printed together on a chip, as is shown in the right panel of figure 2.5. On this chip, several scanners with different dimensions and geometries of the springs and the membrane are made. How the resonance frequency and scan range can be tuned as a function of their geometrical properties is explained in detail in section 2.3.1. Besides altering the geometry, reducing the weight of the scanning membrane (and thereby increasing the resonance frequency) of the scanning membrane can be done by removing part of the structure as shown in the left panel of figure 2.6. Of

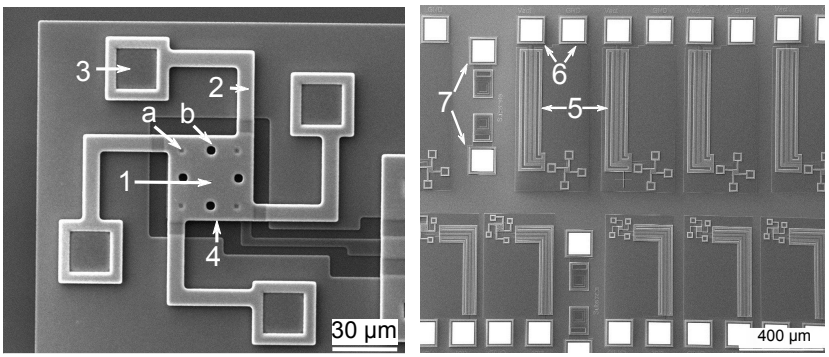

Figure 2.5: Left: *SEM micrograph of the 'standard' MEMS scanner. The scanner consists of (1) a membrane with dimples (a) and etch holes (b); supporting springs (2), fixed at the supports (3); and an actuation plate (4) hidden below the membrane. The STM tip is to be deposited separately, on the central, scanning membrane.* Right: *SEM micrograph showing several MEMS z-actuators on a part of a PolyMUMPS wafer. The scanners have different dimensions of their membranes and supporting springs, and will therefore differ in terms of their resonance frequencies and achievable scan ranges. The actuation lines (5) of the scanners run to the contact pads (6). Also shown, at the left of the image, are two contacting pads which are used for applying a well-defined voltage to the substrate (7).*

course, this also reduces the voltage overlap and therefore alters the actuation properties.

In addition to these spider-leg flexures, there are other scanner designs which combine a high resonance frequency with an acceptable scan range, such as the "fly swatter" scanner shown in the right panel of figure 2.6. This scanner is made with the SOIMUMPs process and has a thickness of 10 μm, making this a very stiff structure. Making use of the through-etch available in the SOIMUMPs process, high-frequency MEMS resonators can be made which could serve as sample carriers providing high-speed in-plane scanning (see the left panel of figure 2.7). This would, however, place severe restrictions on the sample size and mass. Since we want to build a multi-purpose high-speed scanner, we choose not to investigate this route further.

It is also possible to design multidimensional scanners by placing in-plane actuation structures, for instance comb fingers or actuation plates, next to the scan plate. An example of this is shown in figure 2.7. However nice this may seem, the designed structures will have either a very low mechanical resonance frequency due to the large, thin structures, and / or they will have a very small scan range due to the small actuation forces applied. In addition, these scanners will suffer from capacitive coupling between the different scan-

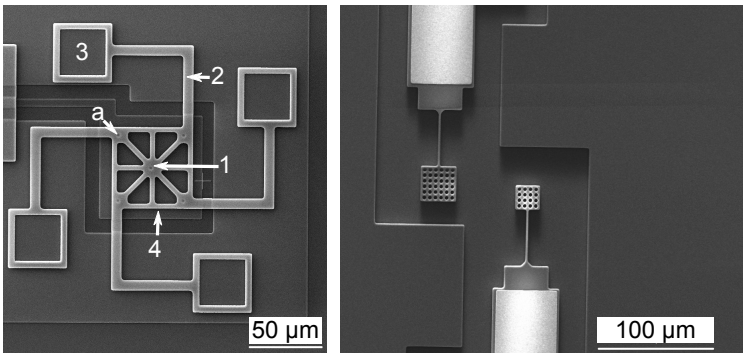

Figure 2.6: Left: *SEM micrograph showing a MEMS STM z-scanner with the scanning membrane (1) with dimples (a), support springs (2), fixed supports (3) and the actuation plate (4). The weight of the scanner is reduced by reducing the area of the scanning membrane, the moving part of the STM.* Right: *SEM micrograph of two fly swatter scanners made with the SOI MUMPS process, aligned in opposite directions. The holes are not only etch holes but are also intended to reduce the weight of the scanner and thereby increase the resonance frequency. They as well reduce the squeeze film damping.*

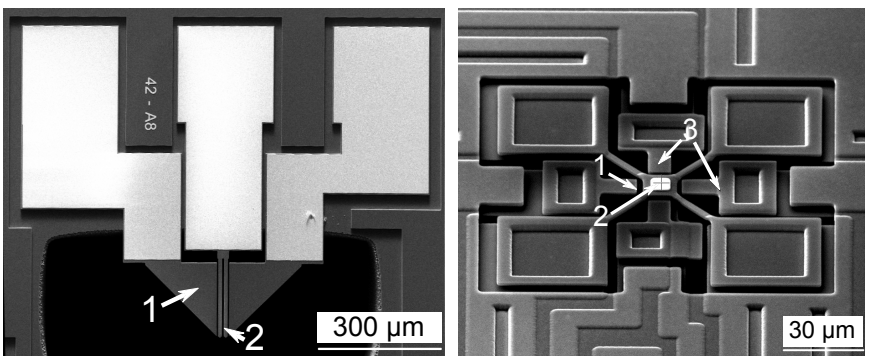

Figure 2.7: Left: *Oscillator made with the SOIMUMPS process. Actuator plates (1) are located next to a tuning-fork like scanner (2). A sample or tip can be deposited on one of the arms, after which the oscillator can be used to perform the fast scan direction.* Right: *3-dimensional MEMS STM scanner made by the PolyMUMPS process. The scanner is displaced out-of-plane by the actuation plate (1) located below the membrane (2); the in-plane motion is governed by the actuation plates located at the sides of the scanner (3).*

ning directions. Therefore, we have first focused on designing one-dimensional scanners. More-dimensional scanners will be discussed in more detail in appendix A.
The two scanners that we have used for to test MEMS STM functionality are of the "spider"-type (as shown in figure 2.5) and the "fly-swatter" type (as shown in figure 2.6).

2.3 Advantages of MEMS in STM systems

In terms of vibrational properties of an SPM scanner, MEMS scanners can exhibit several advantages over scanning piezo elements. In both systems, the resonance frequency is determined by the mass m and the spring constant k: both are high for a piezo element, both are low in a MEMS scanner. In MEMS scanners, it is relatively easy to choose m and k separately, and therefore it is possible to optimize MEMS scanners for high-speed scanning. In addition, MEMS scanners have a smaller mass than piezo elements used in SPM, limiting the induced motion of other components in the mechanical loop from tip to sample. The advantages of incorporating a high-resonance-frequency, low-mass fast-scanning element with a small scanning range on top of a large-range, low-resonance-frequency, and heavy scanning element has been recognized before [33, 59, 60] for the combination of large-range and short-range piezo elements. An additional advantage of MEMS scanners over piezo-based SPM scanners results from the difference in actuation method between piezo elements and MEMS devices. Well-documented errors in piezo motion are caused by creep/hysteresis and fatigue, which occur due to the driving of the piezo element by voltage, instead of charge. These erratic motions do not occur in MEMS devices, as they are actuated electrostatically. This, in the case of MEMS-based STM imaging, should significantly reduce the deformation of the acquired images. Here, we focus on the mechanical properties of a combined MEMS-piezo system.

2.3.1 Resonance frequencies

The resonance frequency of an average tube piezo element with a range of motion of a few micrometers is typically in the order of 10 kHz. For stack piezo elements, the resonance frequency can be as high as 100 kHz. The mechanical loop of an STM scanner is very sensitive to vibrations both from outside and from the scanning piezo element itself.
MEMS scanners can be designed with much higher resonance frequencies than

conventional piezo elements, while the motion of these scanners does not seriously excite the lower-frequency resonances of the scanner body since the mass of a MEMS-scanner is very small compared to that of the other components of the scanner body. In MEMS, as in piezo scanners, there is a trade-off between resonance frequency and scan range. Our uniaxial MEMS z-actuators have fundamental resonance frequencies between 250 kHz and 1.5 MHz (depending on the geometry), while maintaining a scan range in the z-direction in the range of 600 nm to 200 nm. This range is sufficient for many STM experiments, and the MEMS z-actuator can be integrated on top of a piezo element to enable long-range scanning with a hybrid system. This combined geometry is mechanically equivalent to a mass-spring system with 2 springs and 2 masses.
The fundamental resonance frequency of a structure is determined by its spring constant k and its mass m by the relationship

$$f_0 = \frac{1}{2\pi}\sqrt{\frac{k}{m}} \tag{2.4}$$

The spring constant and mass are, in turn, determined by the geometrical properties and the material properties such as the Young's modulus E and the Poisson ratio ν.

For a spider-leg flexure device, such as our MEMS z-actuator the spring constant is given by [50]:

$$k = \frac{2Ew(\frac{t}{l})^3}{2 + 6[(1+\nu)/(1+(w/t)^2]} \tag{2.5}$$

Here, w is the width of the legs, t their thickness and l their length. This formula is valid only for spider-like flexure structures with equally long legs, as is the case in most of our MEMS scanners, especially for all the MEMS scanners that we have used to test the scanning motion. A typical MEMS mass is a few picograms; a typical spring constant is a few N/m. Combining (2.3) and (2.5), we find the position of the membrane as a function of the applied voltage and the geometrical properties of the scanner. In addition, this can be combined with the relationship between fundamental resonance frequency and spring constant (2.4), giving the resonance frequency as a function of geometrical properties. The results of these calculations is shown in figure (2.8). The position of our MEMS device on these curves is indicated. We see that as we increase the resonance frequency of the MEMS by tuning the membrane and spring dimensions, we limit the achievable scan range: there is

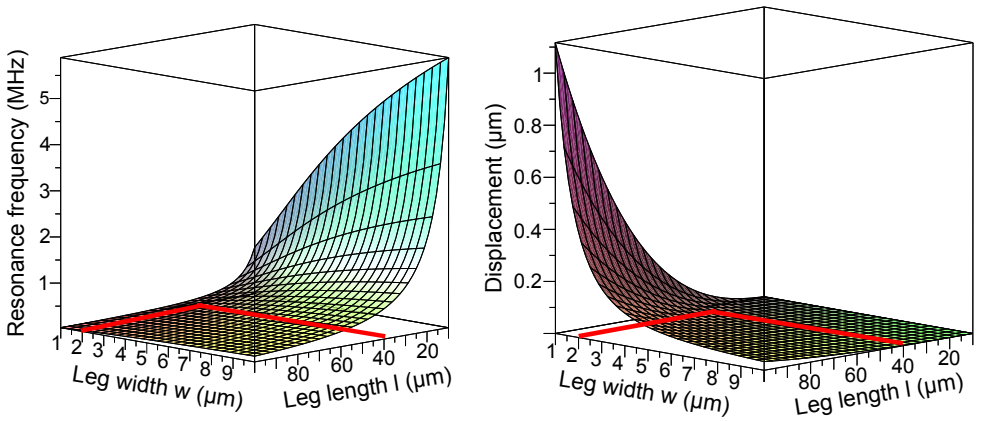

Figure 2.8: *Fundamental resonance frequency (left) and membrane displacement at an actuation voltage of 10 V (right) vs. geometrical properties, calculated analytically for a spider-like MEMS device. The thickness t of the device is fixed to 2 µm, and the membrane is 40 µm x 40 µm. The length l and width w of the legs are variables. The geometry of our MEMS-scanner (l = 40 µm, w = 2 µm) is indicated by the red lines. Note that the length indicates one straight part of the leg structure; i.e. including the corner part the legs length is 2l.*

a trade-off between actuation range and resonance frequency, and the scanner can be optimised depending on the most important property. Fast scanners with a small actuation range can be used for relatively flat samples, while slightly slower scanners with a larger actuation range can be used for rough surfaces, or surfaces with a rapidly changing topography, for instance during surface chemical reactions and phase transitions.

2.3.2 MEMS-piezo hybrid scanning system

Fast piezo-element based scanners need a very rigid mechanical design with a high resonance frequency. The motion of the scanning piezo element can excite resonances in the other mechanical components in the loop from tip to sample, and this will undermine imaging quality and can even lead to tip crashes. A solution for this is to implement a hybrid scanning system. This can consist of a long-range piezo element with a small, high-resonance-frequency piezo element on top, or alternatively of a long-range piezo element with a fast MEMS scanner on top. These hybrid geometries combine the best of two worlds: a slow, long-range scanner that follows slow changes on the surface combined with a fast scanner of limited scan range to track high-

speed changes in height. This type of system has to meet two important requirements:

1. The fundamental resonance frequency of the high-speed device should be sufficiently high to follow all coarse motion performed by the slower scanning element within the allowable error, so that it is not set into motion by the slow scan;

2. The mass ratio between the small scanning element and the larger scanning element needs to be such, that the high-speed motion of the smaller element will not excite resonances of the larger scanning element.

These requirements will be explained more fully in the following sections. The hybrid scanning configuration can be described as a dual mass-spring combination. The theory of these systems is explained, for example, in [61].

Requirement 1: coarse motion and resolution

The minimum required resonance frequency of the MEMS scanner depends on three criteria: the out-of-plane minimum resonance frequency required to image surface features at high speeds, the minimum out-of-plane resonance frequency required to follow out-of-plane coarse motion performed by a piezo element with a maximum position error and the minimum in-plane resonance frequency required to follow the in-plane motion of the piezo element with a maximum position error.

First, the required out-of-plane resonance frequency to image at a certain speed can be calculated as explained in [31]. When acquiring an image of size $L \times L$, at imaging acquisition rate n_i and with $p_i \times p_i$ pixels, the average tip velocity will be

$$V_{tip} = 2Ln_ip_i \tag{2.6}$$

If the atomic structure of the scanned surface has a period λ, the required actuation frequency to image the surface with atomic resolution should be at least:

$$f_a = \frac{V_{tip}}{\lambda} = \frac{2Ln_ip_i}{\lambda} \tag{2.7}$$

For example, if we image a 10 nm $\times$ 10 nm area, with a surface period of 0.25 nm with 512×512 pixels, and we want to image at 25 images per second,

the minimum required feedback bandwidth (and thus, the minimum required resonance frequency of the z-actuator) is 1.024 MHz.

The hybrid MEMS-piezo element system (or for a small piezo element - large piezo element system) can be described as a double mass-spring system: the mass and spring constant of the piezo element are combined with the mass and spring constant of the MEMS membrane and the supports. In turn, the coupling of the entire scanning system of MEMS and piezo element to the rest of the scanner can be described as a system of two masses, coupled by a spring. Here we focus on the MEMS - piezo element combination. The MEMS scanner will follow the piezo motion. Depending on the mass (m_m) and spring constant (k_m) of the MEMS and the frequency of motion (f_p) and amplitude (x_p) of the piezo element, the MEMS will follow the piezo motion with an amplitude error x_{me} given by:

$$x_{me} = \frac{4\pi^2 m_m x_p f_p^2}{k_m} \tag{2.8}$$

With the equation for the resonance frequency (2.4), we find the minimum tolerable value of the natural resonance frequency of the MEMS scanner f_m, for a given combination of the frequency and range of motion of the piezo element and a maximum allowable error in MEMS position:

$$f_m \geq f_p \sqrt{\frac{x_p}{x_{me}^{max}}} \tag{2.9}$$

It is important to realise that there is a difference between relative position accuracy (limited by noise, for instance from the electronics) and absolute position accuracy (limited by, for instance, piezo hysteresis). Relative position accuracy is important to allow imaging with atomic resolution: in order to 'see' atoms, the relative position accuracy should be better than $1/10^{th}$ of the atomic spacing, so better than 0.25 Å. Absolute position accuracy is important to precisely position the tip above interesting positions on the surface. If we demand a minimum absolute position accuracy of the MEMS scanner with respect to the piezo element, this also means that the relative position accuracy will be equal to this minimum absolute position accuracy, or better. Therefore, demanding a minimum absolute position accuracy ensures that the MEMS scanner will follow the motion of the piezo element accurately enough, to allow imaging with atomic resolution. To ensure that imaging with atomic resolution is possible with this hybrid scanning configuration, we set the maximum allowable absolute position error at x_{me}^{max}= 0.1 Å.

For example, let us assume that we have a piezo slowly following large-scale z-features, moving over 10 μm in the z-direction at a frequency of $f_p = 100$ Hz (this is still a relatively large motion at a high speed). To obtain the required resolution, the minimum natural resonance frequency of the MEMS is given by:

$$f_m \geq f_p \sqrt{\frac{x_p}{x_{me}}} = 100 \sqrt{\frac{10^{-5}}{10^{-11}}} Hz = 100 kHz \tag{2.10}$$

The same calculation can also be applied to in-plane motion if we assume sinusoidal scanning. We would like to know the minimum required resonance frequency of the MEMS z scanner in the x,y direction as a function of the number of images per second n_i, if we demand that the MEMS scanner is not the limit on the image quality. We state that the MEMS scanner should not introduce an error greater than the pixel size. A smaller error would not add to the image quality, whereas with a larger error the MEMS will be the limiting factor of the image quality. The line frequency is equal to the motion frequency of the piezo element. If we assume an image size of $p_i \times p_i$ pixels, then $f_p = P_i n_i$. The pixel size is given by the image size, i.e. the travel of the piezo element, divided by the number of pixels, typically $L_{pixel} = \frac{x_p}{512} = x_{me}$. Now we can derive a criterion for the minimum resonance frequency of a MEMS scanner on top of a piezo element:

$$f_{x,ym} \geq p_i n_i \sqrt{\frac{x_p}{x_p/p_i}} = p_i^{3/2} n_i \tag{2.11}$$

We see that the required resonance frequency scales linearly with the image acquisition rate. As an illustration, some numbers are given in table 2.1. For triangular scanning, we would have to take into account the higher-order frequencies: this will limit the achievable imaging rate. Note that we did not take into account any damping. Squeeze film damping, an important factor in MEMS devices, would decrease the position error of the MEMS, caused by the motion of the piezo element. This damping thus would allow MEMS scanners with a lower resonant frequency than required by 2.10 and 2.11 to still follow the piezo motion accurately.
Since the fundamental resonance frequencies of the MEMS are so much higher than the fundamental resonance frequencies of the piezo element, the MEMS scanner will never be disturbed by the piezo motion, even if there is no damping at all.

Image acquisition rate	Minimum resonance frequency of MEMS	
	256 × 256 pixels	**512 × 512 pixels**
1 Hz	4 kHz	11.6 kHz
10 Hz	40 kHz	116 kHz
100 Hz	400 kHz	1.16 MHz

Table 2.1: *Minimum resonance frequency of a MEMS scanner, required to follow the coarse x,y-motion of the scanning piezo element with less than one pixel of distortion.*

Requirement 2: Stability of the mechanical loop during MEMS actuation

The force applied to actuate the MEMS scanner also acts, in the opposite direction, on the piezo element. We can describe the piezo element as a mass-spring system with one fixed side (the side that is glued to the scanner body). This means we have to take into account the effective mass of the piezo element which, in this case, is 1/2 of its total mass. At low frequencies, up to the resonance frequency $f_{0,p}$ of the piezo element, we should expect the strongest response of the piezo element to the actuation of the MEMS, which then satisfies:

$$k_m x_m = -k_p x_p \tag{2.12}$$

Here, the left-hand side is the force due to the MEMS actuation, and the right-hand side is the resulting force on the piezo element. For both piezo element and MEMS scanner we can express the spring constant as a function of natural resonance frequency and mass (2.4), giving:

$$f_{0,m}^2 m_m |x_m| = f_{0,p}^2 \frac{1}{2} m_p |x_p| \tag{2.13}$$

From this, we find the induced piezo motion:

$$|x_p| = \frac{2 f_{0,m}^2 m_m}{f_{0,p}^2 m_p} |x_m| \tag{2.14}$$

For example, we can have a piezo element with a resonance frequency of 100 Hz and a mass of 10 gram, and a MEMS scanner with a resonance frequency of 1MHz. The mass of the MEMS scanner can be estimated as follows: for a scanner with sides of 40 micrometer and a thickness of 2 micrometer, the volume is $3.2 \cdot 10^{-15} m^3$. The mass density of silicon is known to be $2.3 \times 10^3 kg/m^3$, yielding an estimated MEMS mass of $6 \cdot 10^{-12} kg = 6pg$. The MEMS scanner

is used to perform fast, short-lengthscale feedback, for instance over 10 nm. The induced distortion of the piezo element is found to be as small as $10^{-20}m$! To find the distortion when the MEMS is actuated *at* the resonance frequency of the piezo element, we have to multiply this number by the Q factor of the piezo element, which is estimated to be Q=10.000 at the resonance frequency. Even this worst-case induced distortion is only $10^{-16}m$. This is so far below the resolution of any STM scanner that MEMS-induced motion of the piezo element does not introduce restrictions on the design parameters of the STM. Of the entire mechanical loop of the STM scanner, the piezo element will be the element with the highest sensitivity to the motion of the MEMS scanner. MEMS scanner motion can only influence the mechanical loop of the scanner by exciting motion in the piezo element. As we have seen, this effect is negligible, so the image quality will not be disturbed by MEMS-induced vibrations in the mechanical loop from tip to sample. In conclusion, combining a high-frequency, low-range MEMS scanner with a low-frequency, long-range piezo element is beneficial for the high-speed scanning capabilities of the scanning system as a whole due to the large mass mismatch between the heavy piezo element and the light-weight MEMS device.

2.4 State-of-the-art high-speed MEMS SPM

MEMS-based SPM scanners look very promising for high-speed SPM imaging, given the illustrative calculations of section 2.3. MEMS SPM devices have been designed previously by a number of groups, for instance [62–65]. Apart from the development of (miniature) cantilevers with integrated sensors and / or actuators ([66–68]) for AFM purposes, the efforts to develop a MEMS SPM scanner have not led to a widespread use of such scanners to date. The previously developed MEMS scanners typically have dimensions of 100 micrometer wide, hundreds of micrometers to a millimetre long and tens of micrometers thick. These dimensions are not small enough to allow high resonance frequencies. Already in 1990, Akamine, Albrecht et al. [62, 69, 70] published the results on a microfabricated STM. The purpose of making a smaller STM was to decrease the sensitivity to external vibrations and thermal drift, to increase the mechanical resonance frequencies, and to enable batch fabrication of STMs. In that work, a method was described to manufacture arrays of STMs on Si wafers. The actuator mechanism was a bimorph piezoelectric cantilever, 1 mm in length, with alternating layers of metal and piezoelectric material. Atomic resolution on HOPG at 20 frames per second

was demonstrated with that device in constant-height mode. Nevertheless, such devices are nowadays not used in STM measurements and are apparently not the solution for high-speed imaging.
An integrated micro-scanning tunneling microscope with integrated cantilever and tip, a MEMS device, was presented by Xu et al. [64]. They presented two different STM designs, both using comb drive actuators for xy-actuation and a torsional z-actuator; the difference was in the length of the z-actuator. One measured 200 μm, the other 2 mm. The larger STM was equipped with a tip of 20 nm diameter. The smaller STM had a single-crystal silicon tip which was formed by thermal oxidation of silicon. The resonance frequencies of these devices were 5.4 kHz along x and 3.1 kHz along y. With the larger of the two STMs, tunneling on a test sample with 300 nm wide lines was shown.
AFM imaging with a micromachined xy-positioner has been shown by Indermühle et al [71, 72]. This was a constant-height AFM, where four comb drives were used to realise xy-positioning. The wafer was etched through to allow optical detection of the cantilever deflection. The first lateral resonance frequency was determined to be 16 kHz; the first out-of-plane resonance frequency has been found at 13 kHz. AFM imaging has been performed in contact mode on a tungsten carbide needle, with a relatively high noise level compared to imaging with a commercial instrument.
Scanning with a microfabricated array of tips to increase scanning speed has been investigated by several groups, for example by Ahn [73]. Here, each cantilever was equipped with a comb drive for actuation. Imaging of a CNT has been shown with this device. MEMS AFM has also been done with a thermally actuated three-dimensional scanner [74]. This AFM has been used to scan a calibration grating with features 3 μm in-plane and 2 μm out-of-plane at an unspecified speed.
The high-speed capabilities of MEMS SPM have been recognized by Staufer et al. [39], using a comb-drive electrostatic actuator. Using this setup, a piezo surface was imaged with a maximum range of 12 μm at a line rate of 61 Hz. The total bandwidth of the scanner was 80 kHz.
An overview of these efforts is given in table 2.2.
A large part of MEMS SPM design studies has concentrated on high-density data storage applications, the most famous example being the IBM Millipede [75–79]. This has also been investigated by Samsung [80]. None of these designs have made it to commercial applications yet. A significant weakness is the write/read speed of these devices; an optimized MEMS might read/write at a rate of a megabyte/second, while modern hard drives read/write at a gigabyte/second. A related application is the use of arrays of AFM cantilevers

for nanolithography (for example, [81]).
To our knowledge, no high-speed actuated MEMS scanner exists that is routinely used in SPM experiments. It seems that new problems arise when using these small, microfabricated devices to scan a macroscopic sample at atomic resolution. Apparently, the problems associated with making a fully functional MEMS STM z-actuator, which can be integrated into various STM designs and can image the full range of samples that can be imaged by a piezo-based STM, is not yet solved. These problems, along with proposed solutions, will be discussed in the next chapter.

Author	AFM/ STM	Type	Purpose	Image description	Imaging speed
Akamine et al. [69, 70], Albrecht et al. [62]	STM	Piezoelectric cantilever	Decrease sensitivity to external vibrations and thermal drift; increase resonance frequencies; enable batch fabrication	atomic resolution on HOPG	20 frames/s in constant-height
Xu et al. [64]	STM	MEMS; 200μm	High-speed scanning and atom manipulation	no image	Resonance frequency: 5.4 KHz in x, 3.1 kHz in y
Xu et al. [64]	STM	MEMS with integrated tip; 2 mm long	High-speed scanning and atom manipulation	Grating with 300 nm lines	Resonance frequency: 5.4 kHz in x, 3.1 kHz in y
Indermühle et al. [71, 72]	AFM	MEMS; comb drive actuation, no feedback, optical readout	XY-positioning at low drive voltages, accurate vertical detection	imaging on tungsten carbide needle	1st lateral resonance frequency: 16 kHz; 1st out-of-plane resonance frequency: 13 kHz
Ahn et al. [73]	AFM and STM	Array of cantilevers	parallel nanolithography and parallel AFM	Imaging on CNT	Not specified
Vettiger, Liu, Knoll et al. [75, 77, 79]	AFM: IBM Millipede	Array of cantilevers	high-density data storage	Images of written data structures up to 18 nm resolution	Tip thermal response of few μs for read/write
Degertekin, Onaran et al. [37, 38, 82, 83]	AFM	MEMS: FIRAT probe	direct measurement of tip-sample interaction forces	20 nm high steps on calibration grating	10KHz bandwidth; 3.75 frames/s at 16 lines/frame
Akiyama, Staufer et al. [39]	AFM	Cantilever with actuator	high speed	Image of piezo surface; 12 μm range	80 kHz bandwidth; 61 Hz line rate
Chen et al. [84]	'SPM'	MEMS cantilever with actuator	high resolution, large range (150μm×150μm, high speed	no image	No information
Y. Ando [85]	AFM	MEMS 3D comb drive	Low hysteresis, high temperature operation	Image of platinum, approximately 200 nm × 200 nm; no clear resolution	Not specified
Kim et al. [86]	AFM	MEMS membrane	Increased scanning speed	No image	Prediction: resonance frequency = 1.2 MHz
Bay et al. [87]	AFM	Capacitive readout	Increased scanning speed and UHV application	No image	Resonance frequency around 100 kHz

Table 2.2: Overview of recent developments in MEMS SPM technology